Elsevier Editorial System(tm) for Journal of Atmospheric and Solar-Terrestrial Physics
Manuscript Draft

Manuscript Number:

Title: Modelling the midlatitude ionospheric F2-layer for year 2002 with the TIME-GCM coupled model

Article Type: Research Paper

Keywords: Ionospheric modeling; General Circulation Models; Model-Data Comparisons; F-layer Morphology

Corresponding Author: Miss Joei Wroten, B.S.

Corresponding Author's Institution: Boston University

First Author: Henry Rishbeth, Ph.D

Order of Authors: Henry Rishbeth, Ph.D; Michael Mendillo, Ph.D; Joei Wroten, B.S.; Raymond Roble, Ph.D

Abstract: The NCAR Thermosphere-Ionosphere-Mesosphere-Electrodynamics General Circulation Model (TIME-GCM) has been run, using solar-geomagnetic indices for the year 2002, climatological forcing of geopotential height and temperature at the 10 hPa level (28 km height), and forcing by planetary waves and gravity waves transmitted from below. The modelled peak electron density NmF2 matches ionosonde data quite well at five northern mid-latitude sites. It does less well at two southern hemisphere sites, giving excessively high NmF2 in winter associated with high ratios of atomic oxygen to molecular nitrogen, probably related to the patterns of vertical air motion in southern latitudes.

Modelling ionospheric mid-latitudes F2-layer for year 2002 with the TIME-GCM coupled model

H. Rishbeth[a,b] , M. Mendillo[a] , J. Wroten[a,*], R. G. Roble[c]

[a] Center for Space Physics, Boston University, 725 Commonwealth Avenue, Boston, MA 02215, U. S. A.

[b] School of Physics and Astronomy, University of Southampton, Southampton, SO17 1BJ, U. K.

[c] High Altitude Observatory, National Center for Atmospheric Research, Box 3000, Boulder, CO 80307, U. S. A.

hr@phys.soton.ac.uk, mendillo@bu.edu, jwroten@bu.edu, roble@hao.ucar.edu

Abstract: The NCAR Thermosphere-Ionosphere-Mesosphere-Electrodynamics General Circulation Model (TIME-GCM) has been run, using solar-geomagnetic indices for the year 2002, climatological forcing of geopotential height and temperature at the 10 hPa level (28 km height), and forcing by planetary waves and gravity waves transmitted from below. The modelled peak electron density NmF2 matches ionosonde data quite well at five northern mid-latitude sites. It does less well at two southern hemisphere sites, giving excessively high NmF2 in winter associated with high ratios of atomic oxygen to molecular nitrogen, probably related to the patterns of vertical air motion in southern latitudes.

[*] Corresponding Author. Center for Space Physics, Boston University, 725 Commonwealth Avenue, Boston, MA 02215, U. S. A. Tel:+00 1 617 353 2631; fax: +00-1-617-353-6463; E-mail address: jwroten@bu.edu

Keywords: Ionospheric modeling; General Circulation Models; Model-Data Comparisons; F-layer Morphology

1. Introduction

The F2-layer is well known to be the most variable of the normal ionospheric layers. Most of its daily, seasonal and solar-cycle variations are quite well understood, and in principle result from the global circulation in the thermosphere (Rishbeth, 1998), sketched in Fig. 1. Some aspects, such as the day-to-day and hour-to-hour variability of the layer, are not fully understood. Forbes (2000), Fuller-Rowell et al. (2000) and Rishbeth and Mendillo (2001) attempted to evaluate the “solar EUV”, “geomagnetic” and “other” contributions to the day-to-day variability. The “other” component has tentatively been attributed to “meteorological” effects arising in the lower or middle atmosphere, but it is difficult to find firm observational evidence for these influences.

In a previous paper (Mendillo et al., 2002) we used the NCAR Thermosphere-Ionosphere-Mesosphere-Electrodynamics General Circulation Model (TIME-GCM), a self-consistent model of the mesosphere, thermosphere and ionosphere with electrodynamic interactions. The model extends from the upper stratosphere at 10 hPa (28 km) to the upper thermosphere at 500 km. At the lower boundary, it was coupled to the NCAR community climate model CCM3 (Liu and Roble, 2002) to give a composite model extending from the upper stratosphere to the base of the exosphere. The levels of solar and geomagnetic activity were held constant throughout the model year, the only variations being the geographic and seasonal changes of solar zenith angle. We reported that computed F2-layer parameters for seven ionospheric sites showed considerable day-to-day variability, occurring in episodes that differ from one site to another. We deduced that this day-to-day variability stems from the variable forcing by dynamic processes, generated in the lower atmosphere and propagated to the ionosphere as mutually interacting planetary waves, tides and gravity waves.

Rishbeth (2007) set out some aspects of thermospheric and ionospheric behaviour that remain to be understood, though progress on some of these problems has since been made, in particular the so-called 'annual anomaly' (Zeng et al., 2008). Others, such as the semiannual variation of thermospheric temperature with maxima in April and October, the associated semiannual variation of F2 layer height, and day-to-day ionospheric variability would be relevant to this work but are not dealt with here.

The present paper uses a more advanced version of TIME-GCM, and compares the peak electron density NmF2 and ionosonde data for the year 2002 at mid-latitude sites. We concentrate on daytime data, in order to evaluate the model under near photochemical equilibrium and provide some insight into the relative variability caused by solar and geomagnetic forcing and coupling from the lower atmosphere, but present some results for local midnight. We also consider the neutral atomic oxygen/molecular nitrogen concentration ratio near the F2 peak.

We describe in section 2 the model and inputs, compare in section 3 the model outputs with actual F2-layer data for seven sites, and discuss in section 4 the absolute numerical 'calibration' of the noon values of NmF2. We discuss in section 5 possible physical reasons for difficulties in modelling the southern hemisphere, and summarize our conclusions in section 6.

2. TIME-GCM simulations for the year 2002.

2.1 The NCAR TIME-GCM. The TIME-GCM (Thermosphere-Ionosphere-Mesosphere-Electrodynamics General Circulation Model) is a self-consistent coupled model of the upper stratosphere, mesosphere, thermosphere and ionosphere, incorporating aeronomy and dynamics with electrodynamic interactions. It was developed in stages over the past 30 years as the TGCM (Dickinson et al., 1981), TIGCM (Roble et al., 1987. 1988) and TIE-GCM (Richmond et al., 1992), and was extended to the lower atmosphere as TIME-GCM by Roble and Ridley (1994) and Roble (1996). The version used here, called the 'c'-model, extends vertically from 30 to 500 km with spatial resolution of 5° in latitude and longitude and 2 grid points per scale height. The model time-step is 5 minutes. The thermospheric composition, in particular the O/O_2 ratio, has been adjusted by reducing the eddy diffusion coefficient from 90 $m^2 s^{-1}$ to 40 $m^2 s^{-1}$.

At its lower boundary at the 30 hPa pressure level, about 28 km height, the 'c'-model is forced at 24-hour intervals with the global NCEP meteorological model. The zonal and meridional winds at the lower boundary set the planetary wave structure around the globe. On them we superimpose the diurnal and semidiurnal propagating tides derived from the Global Scale Wave Model (GSWM) of Hagan et al. (1999). The present paper compares the 'c'-model results with ionosonde data from seven mid-latitude sites. We defer a more detailed description of the model and the effects of different forcings at the lower boundary.

2.2 Solar, geomagnetic and ionospheric inputs. The model is driven with the daily solar F10.7 flux, 81 day average F10.7 cm flux, and geomagnetic Kp imposed every 3 hours. The solar input uses an empirical solar EUV and UV flux model of Solomon (2000), and the auroral particle input uses the high latitude ion convection model of Roble and Ridley (1987). Plasma flow through the upper boundary still presents an unsolved problem; as in our previous work, we assume an empirical flux of 10^8 cm^{-2} s^{-1}, up by day and down by night.

The ionospheric parameters are the same as in the model used by Mendillo et al. (2002), except that the model of E-layer electron density has been improved by adjusting the low wavelength EUV (<10 nm) and X-ray flux with the aid of newer satellite data.

3. Results for F2-layer peak electron density

3.1 Solar and geomagnetic conditions for year 2002. The solar-geophysical parameters for the year 2002 are plotted in Fig. 2. The solar 10.7 cm flux (top) declined overall during the year from near solar maximum conditions at the beginning to solar medium conditions towards the end, with large 27-day variations caused by localized active regions on the Sun's disk. The other three panels show the daily Ap, Kp and |Dst| indices, the latter two being the numerically greatest values occurring on that day. The geomagnetic indices are typical of solar maximum conditions with maxima in April and October.

3.2 How the peak electron density NmF2 varies with local time. The curves in Fig. 3 show how NmF2 varies with local time. Only six sites are shown here and in later figures, Moscow being omitted as the results are similar to those for Chilton but less complete. Table 1 comments qualitatively on how well TIME-GCM represents the shapes of these curves, and Table 2 on features of the day-by-day variations of noon NmF2 shown in Fig. 4. In both tables the seven sites are listed in decreasing order of geographic latitude. 'Days of year' 1-365 are quoted in the descriptions to the nearest 5 or 10 (with names of months added in places, for convenience). Labels *near* and *far* denote sites 'near to' or 'far from' the longitude of the magnetic pole in their hemisphere; see Rishbeth (1998). We do not discuss storm conditions when very low NmF2 may be observed on some days. The numerical values of NmF2 are discussed in section 4.

3.3 O/N_2 concentration ratios at the noon F2 peak. Fig. 4 shows the day-by-day variation throughout the year of the O/N_2 ratio interpolated to the pressure level at the F2 peak. With a vertical resolution of 0.5 scale height, the maximum resulting error in O/N_2 ratio should be unimportant for present purposes.

3.4 Midnight F2 peak. Fig. 5 shows the night-by-night variation throughout the year of peak electron density NmF2 at local midnight, comprising any residual daytime ionization and contributions from the assumed downward flux of oxygen ions. At all six sites, the modelled NmF2 is too low in the summer half of the year, suggesting that a greater downward flux of O^+ ions is needed in both hemispheres. At the northern sites, the modelled NmF2 has prominent peaks 30-50 days before spring equinox and 30-50 days after autumn equinox, not seen in the data, while at Hobart and Port Stanley midnight NmF2 varies almost in antiphase with noon NmF2 throughout the year. In winter, the model values are similar in magnitude to the data, at least at the northern sites, so the assumed downward flux of 10^8 cm^{-2} s^{-1} seems sufficient to maintain the layer. The variations of O/N_2 concentration ratio resemble those of the modelled NmF2, apart from a few episodes, but we do not make a quantitative comparison. At present we have no general explanation of the behaviour at midnight, and we have yet to study the data at local times either side of midnight.

4. Calibration of the ionospheric model at noon.

Table 4 shows the model/data ratios of noon NmF2 expressed as natural (base e) logarithms. Plus signs imply that model values exceed the ionosonde values.

Omitting the two southern sites because of poor winter results, and Moscow because of four missing months, the average for the remaining four northern sites is 0.17 which corresponds to a factor of 1.18. This means that ‘c’-model values of NmF2 are on average 18% high, which appears remarkably accurate, so the model may be regarded as ‘well calibrated’ in the northern hemisphere. But many individual values in the table exceed 0.3 which corresponds to a factor of 1.35, i.e., model values are 35% high. There are much larger factors (sometimes >3) in local winter at southern sites where the model gives completely wrong month-by-month shapes throughout the winter.

5. Discussion

The general conclusion from section 3 is that, at noon, the TIME-GCM ‘c’-model represents well the daily ‘1-365’ variation of peak electron density NmF2 at higher northern mid-latitudes in Europe and North America, but does less well at lower northern latitudes. At southern latitudes the ‘c’-model is not nearly so good, particularly in winter when it gives excessive values of NmF2 linked to excessively high concentration ratios (O/N_2). At midnight TIME-GCM, with an assumed flux of O^+ ions from above, gives strong peaks of NmF2 near equinox that are not seen in the data. Contrary to how some other models have performed at night, TIME-GCM works reasonably well in winter but fails to maintain the nighttime layer in summer. These conclusions apply to the ‘c’-model, and may not apply in the same way to other versions of TIMEGCM,

It is clear that neutral gas composition, in particular the O/N_2 ratio, holds the key to successful modelling of F2 layer electron density. This ratio largely determines the absolute values of NmF2, and its seasonal changes control the month-by-month variations of NmF2. The excessive O/N_2 ratio and NmF2 in southern winter are most probably caused by errors in representing the global pattern of upwelling and downwelling of air (section 5.1), or in eddy diffusion (section 5.2).

5.1 Vertical flow of the neutral air. Fig. 1 illustrates the general pattern of upwelling and downwelling envisaged by Duncan (1969). We suggest that the excessively large atomic/molecular (O/N_2) concentration ratios and consequent high NmF2 at Hobart and Port Stanley, shown in Fig. 4, occur because our version of TIME-GCM places these sites within the winter zone of neutral air downwelling. The more modest values of NmF2 actually observed imply that these sites are north of the zone of strong downwelling. That is consistent with the rather high values of NmF2 observed in winter at Kerguelen in the South Indian Ocean at 49°S, 70°E (Zou et al., 2000), which suggest this site is in the downwelling zone. Furthermore, perusal of three solar cycles of midwinter (June) data from Faraday, in the Antarctic peninsula at 65°S, 64°W, shows that monthly mean NmF2 lies in the range 2-8 x 10^5 cm^{-3} at noon, higher than might be expected with the noonday sun virtually on the horizon and suggesting that the downwelling zone extends far enough south to include Faraday. Some day-to-day changes at Hobart and Port Stanley may be linked to day-to-day changes in the latitude of the auroral oval and downwelling zone.

The auroral model used in TIME-GCM, kindly supplied by A. G. Burns (private communication) shows both Hobart and Port Stanley well north of the equatorward edge of the auroral oval at local noon, 02 UT at Hobart and 16 UT at Stanley. Port Stanley is in the ‘Weddell Sea anomaly’, a region of complex behaviour (Bellchambers and Piggott, 1958).

The CTIPM model used by Zou et al. (2000) reproduces quite well the month-to-month variations of NmF2 at Hobart, Port Stanley and Kerguelen, implying that its model of the southern auroral oval is good. Its June winter downwelling zone in western longitudes extends from about 65°S to 90°S, well south of Port Stanley, and in eastern longitudes lies well south of Hobart (Rishbeth and Müller-Wodarg, 1999).

5.2 Eddy diffusion. Eddy diffusion plays a large part in controlling the O/N_2 ratio and it is important though difficult to compute it correctly. In the earlier TIE-GCM model, eddy diffusion is specified at the lower boundary, but in TIME-GCM it is calculated from the flux of gravity waves transmitted upward through complex wind distributions from the base of the model to the turbopause. Increasing eddy diffusion causes more O to be transported downward and more N_2 upward. Wave activity is strong in southern winter and, although some studies suggest that a low diffusion rate of 40 m^2 s^{-1} exists in winter, others suggest a value of 100 m^2 s^{-1}. The larger rate would reduce the O/N_2 concentration ratio and thus NmF2.

6. Conclusion

The TIME-GCM coupled 'c'-model' reproduces midday NmF2 well throughout year 2002 at seven mid-latitude sites, except for winter in the southern hemisphere. The key to success is correct representation of the neutral air composition in the thermosphere. At midnight the model is not so successful.

In section 4 we discussed the absolute values of NmF2, month by month and site by site, arriving at an overall 'calibration factor' of 1.18 for TIME-GCM in the northern hemisphere. This implies that the model values exceed observed values on average by 18%, a quite accurate performance. Greater inaccuracies are found in the southern hemisphere, notably in winter, associated with unrealistically high atomic/molecular (O/N_2) concentration ratios. The difficulties with neutral composition may be related to eddy diffusion, or to the large scale pattern of vertical motions of the neutral air 'upwelling' and 'downwelling', which are clearly major questions for quantitative study.

Getting these processes right in southern hemisphere winter should bring the peak electron density NmF2 into agreement with the ionosonde data. Apart from the problem in southern winter, the annual and semiannual variations of NmF2 are well explained.

Other topics for future discussion are the day-to-day variability of F2-peak electron density and the seasonal variation of thermospheric temperature, with maxima shortly after the equinoxes. We also draw attention to the problem posed by the semiannual variation of F2 peak height hmF2, which is related to thermospheric temperature. Up to now, TIME-GCM and other coupled models have signally failed to reproduce these well established semiannual characteristics. We have yet to see any critical discussion of this question. Thermospheric modelling is not complete, but it has come a long way!

Acknowledgments

We are most grateful to Ben Foster for his assistance with the TIME-GCM calculations and for providing model output for comparison with ionosonde data, and to Alan Burns for the use of his model of the auroral ovals. We thank the World Data Centres A and C1 for Solar-Terrestrial Physics at Boulder, Colorado, and Chilton, UK, for supplying data. At Boston University, support for this study was provided by a grant from the Aeronomy Program of the US National Science Foundation (NSF). The NCAR modelling efforts are supported by grants from the NSF.

References

Bellchambers, W. H., Piggott, W. R., 1958. Ionospheric measurements made at Halley Bay. Nature 182, 1596-1597.

Dickinson, R. E., Ridley, E.C., Roble, R. G., 1981. A three-dimensional general circulation model of the thermosphere. Journal of Geophysical Research 86, 1499-1512.

Duncan, R. A., 1959. F-region seasonal and magnetic storm behaviour. Journal of Atmospheric and Terrestrial Physics 31, 59-70.

Forbes, J. M., Palo, S. E., Zhang, X, 2000, Variability of the ionosphere. Journal of Atmospheric and Solar-Terrestrial Physics 62 685-693.

Fuller-Rowell, T. J., Codrescu, M., Wilkinson, P., 2000. Quantitative modelling of the ionospheric response to geomagnetic activity. Annales Geophysicae 18, 766-781.

Hagan, M. E., Burrage, M. D., Forbes, J. M., Hackney, J., Randel, W. J., Zhang, X., 1999. GSWM-98: Results from migrating solar tides, Journal of Geophysical Research 104(A4), 6813-6828.

Hedin, A. E., 1987. The MSIS-86 thermospheric model. Journal of Geophysical Research 92, 4649-4662.

Liu, H.-L., Roble, R. G., 2002. A study of a self-generated stratospheric sudden warming and its mesospheric/lower thermospheric impacts using coupled TIME-GCM/CCM3, Journal of Geophysical Research 107(D23), 4695, doi:10.1029/2001JD001533.

Mendillo, M., Rishbeth, H., Roble. R. G., Wroten, J., 2002. Modelling F2-layer seasonal trends and day-to-day variability driven by coupling with the lower atmosphere. Journal of Atmospheric and Solar-Terrestrial Physics 64, 1911-1931.

Richmond, A. D., Ridley E.C., Roble, R.G., 1992. A thermosphere/ionosphere general circulation model with coupled electrodynamics. Geophysical Research Letters 19, 601-604.

Rishbeth, H., 1998, How the thermospheric circulation affects the ionospheric F2-layer. Journal of Atmospheric and Solar-Terrestrial Physics 60, 1385-1402.

Rishbeth, H., 2007. Thermospheric targets, EOS/Transactions of the AGU 88, 189 & 193.

Rishbeth, H., Mendillo, M., 2001. Patterns of ionospheric variability. Journal of Atmospheric and Solar-Terrestrial Physics 63, 1661-1680.

Rishbeth, H., Müller-Wodarg, I.C.F., 1999. Vertical circulation and thermospheric composition: a modelling study. Annales Geophysicae 17, 794-805.

Roble, R. G., 1996. The NCAR Thermosphere-Ionosphere-Mesosphere-Electrodynamics General Circulation Model (TIME-GCM). In: Schunk, R. W. (Ed.), STEP Handbook of Ionospheric Models. Utah State University, pp. 281-288.

Roble, R.G., 2000. On the feasibility of developing a global atmospheric model extending from the ground to the exosphere. Geophysical Monograph, Vol. 123, American Geophysical Union, Washington DC, pp. 53-67.

Roble, R. G., and E.C. Ridley, 1987. An auroral model for the NCAR thermosphere general circulation model (TGCM). Annales Geophysicae 5A, 369-382.

Roble, R. G., and E.C. Ridley, 1994. A thermosphere–ionosphere–mesosphere–electrodynamics general circulation model (TIME-GCM): equinox solar cycle minimum simulations (30–500 km). Geophysical Research Letters **21**, 417-420.

Roble, R.G., Dickinson, R. E., Ridley, E. C, 1987. On the global mean structure of the thermosphere. Journal of Geophysical Research 92, 8745-8758.

Roble, R. G., E.C. Ridley, A.D. Richmond and R.E. Dickinson, 1998. A coupled thermosphere/ionosphere general circulation model. Geophysical Research Letters 15, 1325-1328.

Zou, L., Rishbeth, H., Müller-Wodarg, I. C. F., Aylward, A. D. Millward, G. H., Fuller-Rowell, T. J., Idenden, D. W., Moffett, R. J., 2000. Annual and semiannual variations in the ionospheric F2-layer. I: a modelling study. Annales Geophysicae 18, 927-944.

Table 1 **Comments on shapes of daytime variations of NmF2 vs local time (Fig. 3).**

Moscow 56°N 37°E	Model shapes are very good on the whole, but omit the forenoon peaks (08-10 LT) in spring, especially April, and tend to fall off too quickly at dusk in Mar-Sept.
Chilton 52°N 2°W	Very much as for Moscow, but with forenoon peaks more marked during Jan-Apr.
Wakkanai 45°N 142°W	Model shapes match the data badly, particularly in the winter half of the year (Jan-Mar, Sept-Dec), when data values fall off much faster in the afternoon than do the model values.
Wallops Is 39°N 77°W	In many months the shapes match well, but the forenoon peaks tend to occur later in the model than in the data.
Eglin 30°N 87°W	Daytime peaks in the model occur 2-4 hours too late in every month.
Hobart 43°S 147°E	Model shapes match the data quite well, though with bad mismatches in actual values. Model values fall too quickly after sunset, especially in summer (Jan-Mar).
P Stanley 52°S 58°W	The daytime peaks mostly occur 2-4 hours too late, though in southern winter the model/data mismatch is too great for meaningful comparison.

Table 2 **Comparisons of model with data for noon NmF2 (Fig. 4).**

Moscow 56°N *near*	No data June or Oct-Dec (days 150-180, 270-365). Data have sharp peak around day 30 (Feb) not shown by model. Model values are ~25% too low on most days 70-140 (Mar-May).
Chilton 52°N *near*	Data peak around day 30-35 (Jan-Feb) and have nearly flat minimum days 150-230 (June-Aug). Model is very good in January and March-September, apart from a few days, but fails to show the very high NmF2 on days 20-50 (February). On days 290-350 (Oct-Dec), model values ~10% too high most days, but show big reductions on days 275-280 (storm Kp 7) and some other disturbed days.
Wakkanai 45°N *far*	Data values peak at days 30-35 (Feb) and 300-330 (Nov). Model values are good much of year, but are ~20% too high at the Feb peak and days 200-300 (July-Sept).
Wallops Is. 39°N *near*	Data values are surprisingly almost flat throughout Jan to early Apr (days 1-100), but the model shows sharp Feb peak around days 30-35. Model fits data well for rest of year, but is 15-20% high on days 310-350 (Nov-Dec).
Eglin 30°N *near*	No data days 225-260 (Aug-Sept). Fairly good fit overall, but model is ~25% low on days 70-135 (Mar-May) and ~15% too high on days 280-330 (Oct-Nov).
Hobart 43°S *near*	No data days 305-365 (Nov-Dec). Model values are good on days 1-110 (Jan-Apr) and 270- 300 (Oct), but are much too high throughout winter days 120-270 (May-Sept). The model shows peaks around days

	130 and 200-230, of which the data show little trace, There are many individual days, especially early in the year, with very low data values.
P Stanley 52°S *far*	Data show a basic semiannual variation, peaking in autumn at days 90-100 (April) and in spring (days 260-310 (Sept-Oct). In the model, the autumn peak at days120-150 is too late and the spring peak at days 210-230 is much too early, and is perhaps merged with a spurious winter peak which is not in the data. Model values are ~30% too high in summer, days 1-100 and 276-365.

Table 3 **Comparisons of model and data for midnight NmF2 (Fig. 5).**

Moscow 56°N *near*	No data June or Oct-Dec (days 150-180, 270-365. Data show flat peak in summer (days 80-210), tailing off towards day 270 (late Sept). Model values are too low and flat throughout this period.
Chilton 52°N *near*	Data show flat peak in early summer (days 70-190) tailing off towards day 270 (late Sept). Model values are too low throughout this period, with flat minimum days 110-230 (Apr-Aug).
Wakkanai 45°N *far*	Data show a summer plateau, days 100-280 (Apr-Oct). Model values are much too low and flat in winter, days 100-230 (Apr-Aug) with very marked spring/autumn peaks, less marked in the data.
Wallops Is. 39°N *near*	Data are rather flat throughout year, slightly raised at days 110-230 (Apr-Aug) with many individual values well above the others. Model values flat during summer with marked Feb-Mar and Oct peaks.
Eglin 30°N *near*	Data rise sharply days 1-90, peak in early summer at days 120-150 (May), slowly decline during days 150-310 (June-Oct), stay flat till year end. Model variation very similar to Wakkanai.
Hobart 43°S *near*	No data days 305-365 (Nov-Dec). Data show nearly flat winter minimum (days 140-220), model values are too high; but on summer-autumn days 1-100, model values much below data values.
P Stanley 52°S *far*	Data peak in late summer (days 10-30) and in early summer (days 310-340), sloping down in autumn to flat minimum in winter (days 150-200)

and sloping up in spring. Model varies completely in antiphase with data, with very low values in summer (days 1-60, 300-365), peaks in autumn and spring, trough in winter.

Table 4. **Month-by-month calibrations between model and data.**

Each entry gives the monthly average of the daily ratios, expressed as the natural log of noon NmF2 (model)/NmF2 (data).

2002	**Chilton**	**Wallops I**	**Wakkanai**	**Eglin**	**Mean**
Jan	-0.01	0.36	0.05	-0.34	0.01
Feb	0.23	0.49	0.24	-0.01	0.24
Mar	0.01	0.30	0.11	-0.11	0.08
Apr	-0.20	-0.04	-0.09	-0.06	-0.10
May	-0.28	0.09	0.05	-0.20	-0.09
June	-0.06	0.08	0.15	0.07	0.06
July	0.04	0.33	0.32	0.37	0.26
Aug	0.12	0.42	0.54	0.34	0.35
Sept	0.07	0.35	0.66	0.18	0.32
Oct	0.33	0.26	0.52	0.32	0.36
Nov	0.34	0.26	0.28	0.25	0.28
Dec	0.21	0.30	0.33	0.24	0.27
Mean	0.06	0.27	0.26	0.09	0.17

Figure Captions

Fig. 1 Sketch of the thermospheric circulation, after Rishbeth (1998). The figure represents average conditions in June at around 300 km at no particular longitude. The bold dashed lines at the top and bottom represent the auroral ovals, the dash-dot curve represents the sunrise/sunset terminator, thin dotted lines represent typical isobars, and arrows represent wind directions (but not magnitudes). The upward pointing triangle at 14 LT shows the position of maximum temperature and pressure; the downward pointing triangle at 03 LT shows the position of minimum temperature and pressure. Note that the six hours 00-06 LT are repeated on the right-hand side.

Fig. 2 Solar F10.7 cm flux and geomagnetic indices Ap max and |Dst| max for 2002, ‘max’ denoting the numerically greatest value occurring on the UT date.

Fig. 3 Daytime NmF2 vs local time for twelve months at six sites. The black curves are the daily curves computed from the model. The red shading shows the observed monthly mean NmF2 ± 1 standard deviation. Ideally, two-thirds of the model curves should lie within the red shading.

Fig. 4 Noon NmF2 on days 1-365 for six sites: ionosonde data and ‘c’-model, and noon O/N_2 ratio on the pressure level nearest the F2 peak.

Fig. 5 Midnight NmF2 on days 1-365 for six sites: ionosonde data and ‘c’-model, and noon O/N_2 ratio on the pressure level nearest the F2 peak.

Figure1 - tiff format
Click here to download high resolution image

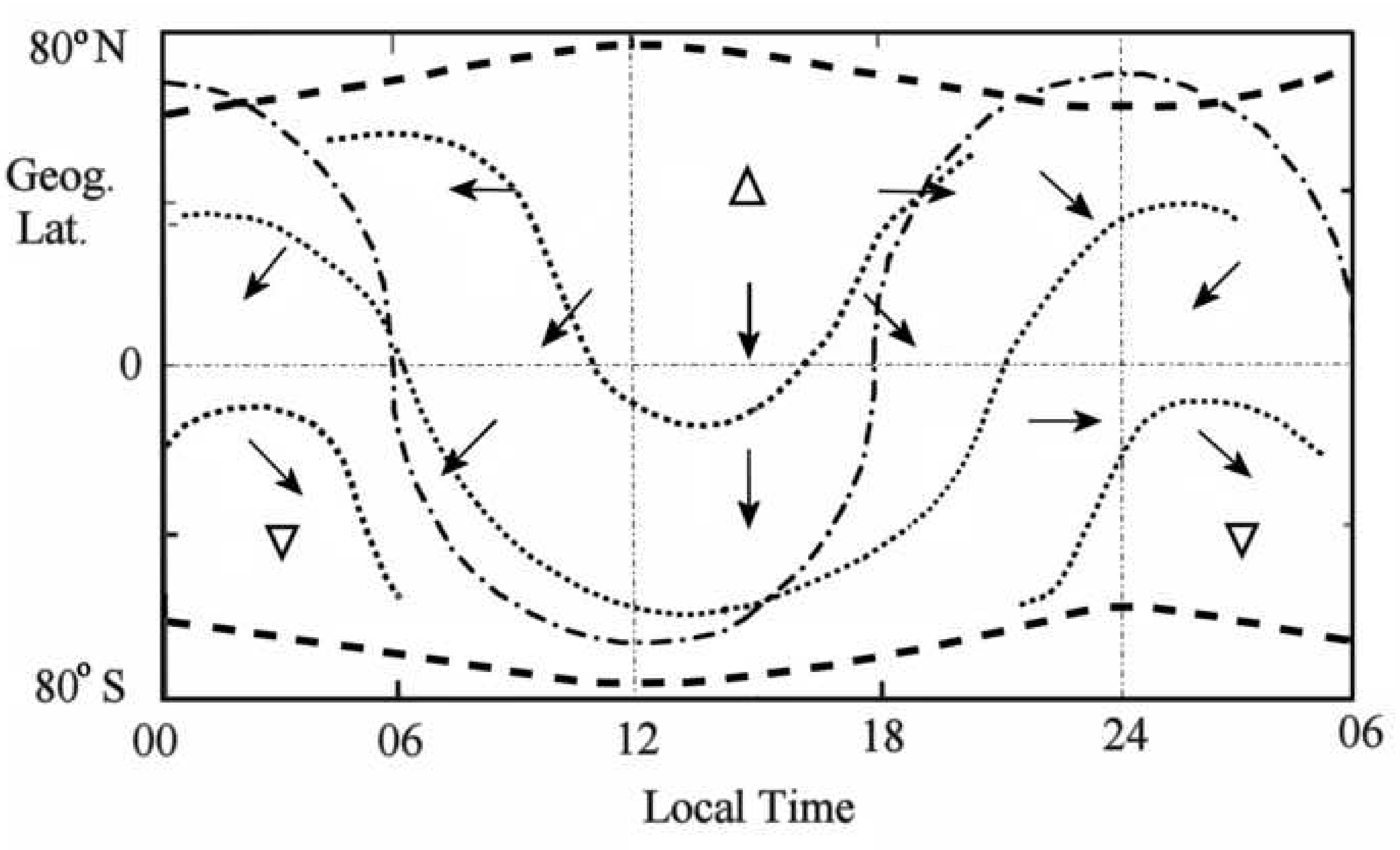

Figure2 - tiff format
Click here to download high resolution image

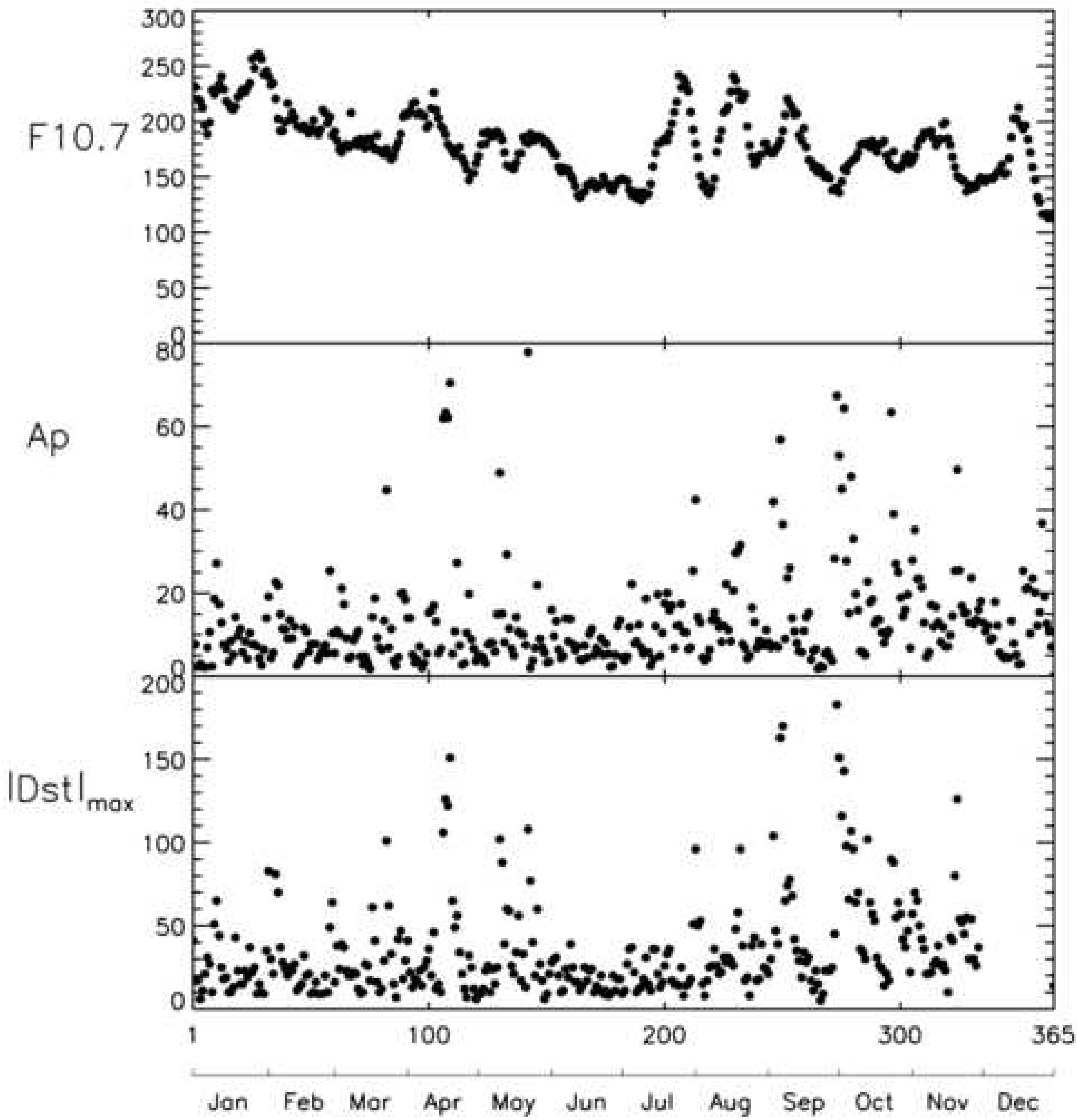

Figure3 - tiff format

Click here to download high resolution image

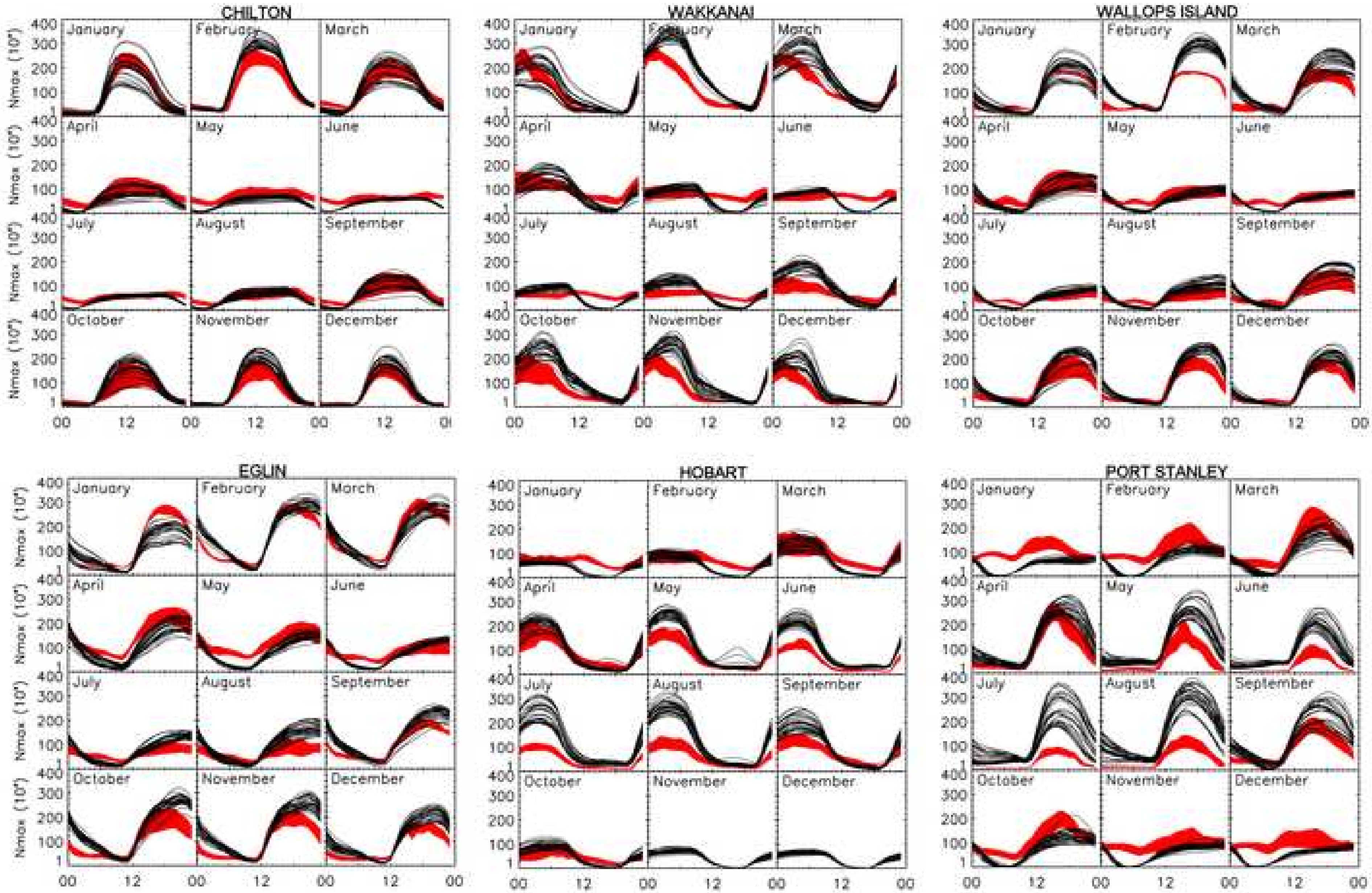

Figure4 - tiff format

Click here to download high resolution image

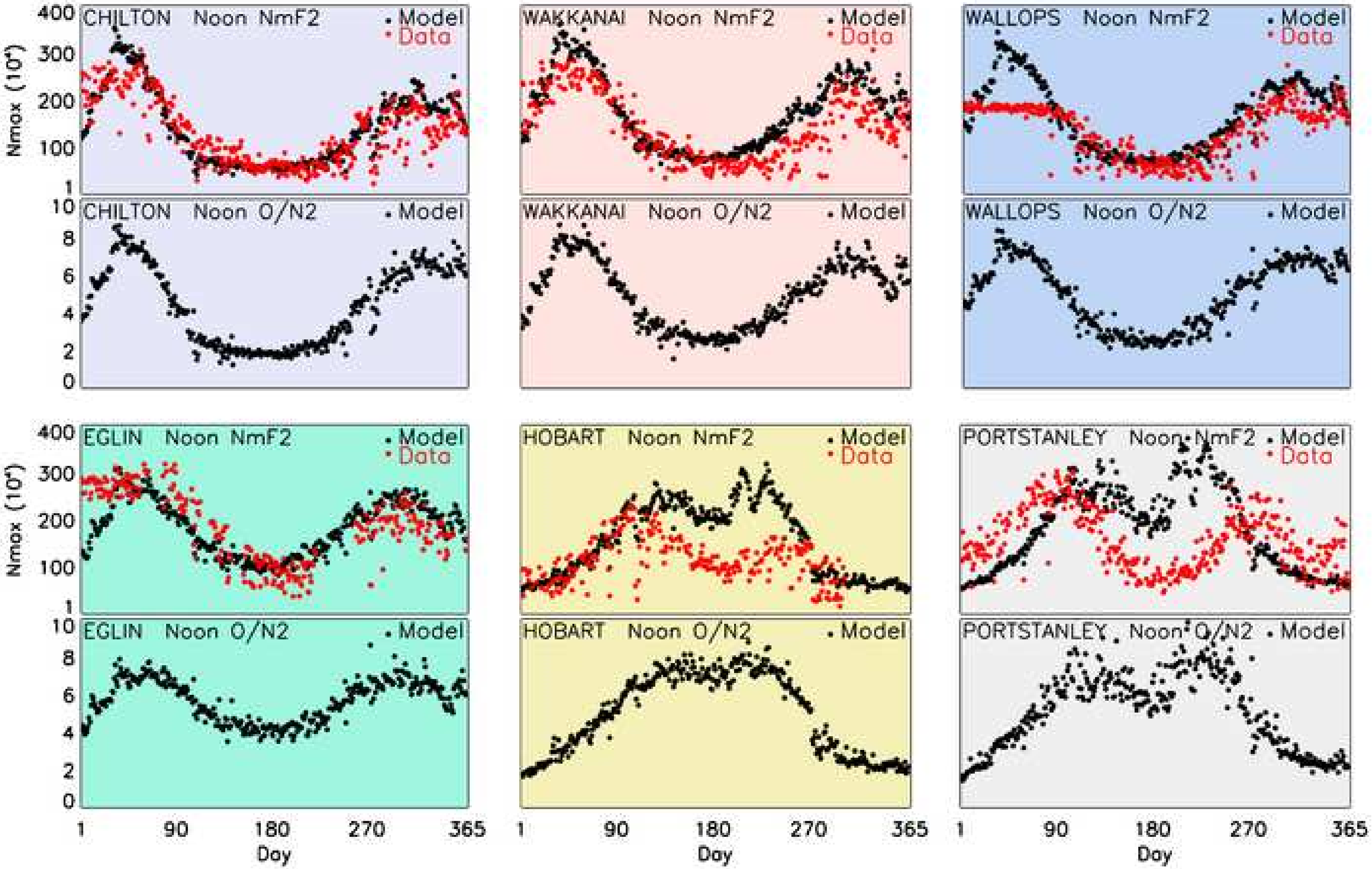

Figure5 - tiff format

Click here to download high resolution image